

Title Page:

Vascular calcification has a role in acute non-renal phosphate clearance

Turner; Role of Vasculature in Acute Phosphate Clearance

Mandy E Turner¹, Austin P Lansing¹, Paul S Jeronimo MSc¹, Lok Hang Lee¹, Bruno A Svajger PhD¹, Jason GE Zelt PhD^{2,3}, Martin P Petkovich PhD¹, Rachel M Holden MD^{1,4}, and Michael A Adams PhD¹

¹Department of Biomedical and Molecular Science, Queen's University, Kingston, ON, Canada

²Department of Cellular and Molecular Medicine, Faculty of Medicine, University of Ottawa, Ottawa, Canada

³Division of Cardiology, University of Ottawa Heart Institute and University of Ottawa, Ottawa, Canada

⁴Department of Medicine, Queen's University, Kingston, ON, Canada

Corresponding Author:

Dr. Michael A Adams

Department of Biomedical and Molecular Sciences

Queen's University

Kingston, ON

K7L 3N6

Tel: 613-533-2985

adams@queensu.ca

Word Count for Manuscript Body: 4908

1 **Abstract**

2

3 **Background:** Non-renal extravasation of phosphate from the circulation and transient
4 accumulation into tissues and extracellular fluid is a regulated process of acute phosphate
5 homeostasis that is not well understood. Following oral consumption of phosphate, circulating
6 levels normalize long before urinary excretion has been completed. This process is particularly
7 critical in the setting of chronic kidney disease (CKD), where phosphate exposure is prolonged
8 due to inefficient kidney excretion. Furthermore, CKD-associated dysregulation of mineral
9 metabolism exacerbates pathological accumulation of phosphate causing vascular calcification
10 (VC). In the present study, the objective was to determine whether the processes involved in the
11 development and progression of VC are also normally involved in the systemic acute response to
12 oral phosphate.

13

14 **Methods:** Acute circulating and physiological phosphate movement and tissue deposition was
15 assessed in two experimental rat models of VC using radio-labelled phosphate challenge. In an
16 adenine-induced model of CKD, VC was induced with high dietary phosphate. Animals were
17 euthanized 2 and 6 hours after oral consumption of radiolabelled phosphate. A non-CKD model
18 of VC was induced with 0.5ug/kg calcitriol and then withdrawn, and radiolabelled phosphate
19 was then given to assess for vascular preference for phosphate uptake with and without the
20 presence of an active calcification stimulus. Samples of 50 different tissues were collected to
21 assess tissue accumulation of *de novo* phosphate in response the challenges.

22

23 **Results:** Animals with CKD and VC have a blunted elevation of circulating $^{33}\text{PO}_4$ following oral
24 phosphate administration and the discordant deposition can be traced to the calcifying
25 vasculature. Deposition of *de novo* phosphate is present until at least 6 hours, which after active
26 gut absorption. The accrual is stimulated by a phosphate challenge, and not present in the same
27 degree during passive disposition of circulating phosphate. The extent of new transport to the
28 calcifying vasculature correlates to the pre-existing burden of calcification, and can be
29 substantially attenuated by removing the stimulus for calcification.

30

31 **Conclusions:** Our data indicate that calcifying arteries alter the systemic disposition of a
32 phosphate challenge and acutely deposit substantial phosphate. This study supports the
33 importance of diet as it relates to acute fluctuations of circulating phosphate and the importance
34 of bioavailability and meal-to-meal management in CKD patients as a mediator of cardiovascular
35 risk.

1 **Introduction**

2 Medial vascular calcification (VC) is a pathology associated with aging, and is
3 accelerated by diabetes and chronic kidney disease (CKD). In these conditions, hydroxyapatite,
4 the predominant storage molecule for calcium and phosphate in bone, is actively formed in the
5 media and elastic lamina of muscular arteries. This pathology reduces vascular compliance,
6 occurs in conjunction with substantial vascular inflammation, and associates with poor
7 cardiovascular outcomes^{1,2}. Phosphate dysregulation has emerged as an important factor in the
8 initiation and propagation of this process and serum phosphate, even in the upper ranges of
9 normal values and at each stage of CKD, is recognized as an independent risk factor for
10 cardiovascular disease³. Prevalence of VC in the thoracic aorta ranges from 37-60% in patients
11 with stage 3 CKD when serum phosphate still within the normal range⁴.

12 Despite the growing recognition of circulating phosphate as a risk factor, less than 1% of
13 total body phosphate content is found in the circulation. The tight regulation of circulating
14 phosphate involves controlled flux within and between several compartments. These pools of
15 phosphate have normally included intestinal absorption of dietary phosphate, the movement of
16 phosphate between skeletal, soft tissue and extracellular pools, and regulation of renal
17 reabsorption and excretion. Phosphate transport in and out of these compartments is mediated, in
18 part, through sodium phosphate-cotransporters (NaPi), as well as ubiquitous somatic phosphate
19 inorganic transporters, PiT-1 and PiT-2. The activity and expression of NaPis are largely
20 regulated by parathyroid hormone (PTH), fibroblast growth factor 23 (FGF-23) and calcitriol.
21 Though not well understood, another mechanism of phosphate movement is the paracellular
22 transport of phosphate along a concentration gradient, an aspect of phosphate disposition which
23 may be underestimated in CKD. Despite the clear role of phosphate in stimulating adaptive

1 changes in its own regulation, the cellular mechanism(s) of phosphate-sensing remain poorly
2 understood in somatic tissues.

3 As kidney function declines, hormonal control mechanisms become unable to
4 compensate and the resultant increase in circulating phosphate stresses cellular mechanisms of
5 phosphate handling. The rise in circulating phosphate can occur acutely after a meal or, in later
6 stages of CKD, present as chronic hyperphosphatemia. Our previous work indicates that acute
7 responses to oral phosphate are already altered in mild to moderate CKD patients with normal
8 serum phosphate⁶. Specifically, challenge compared to those with health kidney function
9 individuals with impaired kidney function but normal serum phosphate had a blunted elevation
10 in their circulating phosphate following an oral phosphate. This attenuated rise suggested that
11 there were changes in the systemic distribution of the oral phosphate load in those with impaired
12 kidney function, but did not provide evidence of the mechanism for this increased non-renal
13 clearance.

14 In a recent study using a rat model of CKD, the impact of oscillating from high to low
15 dietary phosphate every two days resulted in VC much more severe than rats fed the same
16 amount of phosphate without oscillations⁷. The burden of VC was comparable to that found in
17 rats fed a continuously high dietary phosphate containing twice the overall amount of the
18 oscillating burden. These findings suggest spikes in circulating phosphate may be an important
19 driver of VC, potentially more important than overall exposure.

20 There is little evidence for how a given tissue or organ is involved in the systemic
21 disposition of phosphate following administration of an oral load, or how these processes are
22 altered during the development of VC. In the present study, the objective was to determine whether

1 the processes involved in the development and progression of VC are also involved in altering the
2 systemic response to oral phosphate using two animal models of VC.

3

4 **Methods**

5 All animal procedures were performed in accordance with the Canadian Council on Animal Care
6 and were approved by Queen's Animal Care Committee. Male Sprague Dawley rats (15-16
7 weeks, Hilltop Lab Animals Inc. PA, USA) were acclimated for a week prior to the start of the
8 experiment and were individually housed and maintained on a 12-hour light/dark cycle
9 throughout the duration of the study.

10

11 *Adenine-Induced CKD Model of Vascular Calcification* A chronic reduction in kidney function
12 was induced using a 0.25% dietary adenine model for 5 weeks as previously described⁸ (Harland
13 Teklad, TD.08672). A parallel control arm was completed concurrently without the dietary
14 adenine, but otherwise identical diets (CON). After cessation of the adenine diet, animals were
15 maintained on the non-adenine 0.5% phosphate diet for at least 4 days to ensure removal of the
16 acute effects of dietary adenine (TD.150555), and then, at the sixth week, CKD and CON rats
17 were stratified into high or low dietary phosphate according to bodyweight, circulating calcium
18 and phosphate. The low dietary phosphate group remained on the 0.5% dietary formulation (LP)
19 and the high dietary phosphate (HP) increased to 1% dietary phosphate (TD.08670). Blood was
20 collected at least weekly from the saphenous vein. The total number of animals in each group
21 are: CON-LP (N=13), CON-HP (N=11) CKD-LP (N=23) and CKD-HP (N=23).

22

1 *Administration of Oral Radiolabelled Phosphate:* Two weeks following stratification into the
2 dietary phosphate arms, animals were euthanized following an oral radiolabelled phosphate.
3 Animals were partially-fasted overnight to ensure consistency of stomach contents and then in
4 the morning, animals were provided 2mL of sucralose gel (MediGel®, Clear H₂O) with a total
5 phosphate amount of 0.1g (equivalent to 100% daily intake of the LP animals, or 50% daily
6 intake of HP animals). Phosphate in the gel was supplemented with dibasic and monobasic
7 sodium phosphate salts (Sigma-Aldrich, Canada) and ~7.76 million Bq radio-labeled ³³PO₄
8 (NEN Radiochemicals). Animals were stratified by the three most recent measurements of serum
9 creatinine, phosphate, calcium and bodyweight into one of three sacrifice times following the
10 oral load of phosphate: 0 hour, 2 hours or 6 hours. Stratification metrics and final study animal
11 numbers for each time point are outlined in Supplementary Table 1. Depending on sacrifice
12 time, animals were sampled from the saphenous vein at 0, 20min, 40min, 1hr, 1.5hr, 2hr and then
13 hourly until 6hr. Only two rats in the CKD-LP diet presented with VC and both animals were
14 allocated *a priori* to the 6hr sacrifice time point. As a result, animals were excluded from
15 analysis in Figures 2-3, as inclusion would have biased the vascular phosphate deposition
16 findings for 6hr (but not 2hr) in CKD-LP animals.

17
18 *Non-CKD Calcitriol-Induced Model of Vascular Calcification:* VC was induced through
19 subcutaneous administration of suprapharmacological calcitriol (0.5µg/kg/day, Sterimax) for 8-
20 days and maintained on a 0.75% phosphate diet (Harland Teklad, TD.160324). A parallel control
21 arm was completed concurrently. At day 7, animals (N=24) were stratified based on serum
22 calcium, phosphate, PTH, FGF-23 and bodyweight into two time-points. The first group was
23 sacrificed on experimental day 9, following 8 doses of calcitriol (Cx) or controls. The remaining

1 rats no longer received calcitriol (and controls) for 13 days (Post-Cx). The number of animals in
2 each group were: Cx (N=8), Post-Cx (N=9), Control Early (N=3), and Control Late (N=4).
3 Blood was collected every 2-3 days via saphenous vein.

4
5 *IV Radiolabelled Phosphate Administration* Directly prior to sacrifice, animals were
6 administered an intravenous load of radiolabelled phosphate. Intravenous delivery was chosen to
7 bypass the potential effects of supraphysiologic calcitriol on gut phosphate transport. Under
8 isoflurane anesthesia (2.5%, 2% O₂), rats were administered 3mL of an isotonic sodium
9 phosphate/sodium chloride solution containing 300μmol of phosphate and ~9.7 million Bq of
10 ³³PO₄ (NEN Radiochemicals, Perkin Elmer) was infused intravenously into the jugular vein over
11 10 minutes (KD Scientific). Blood was sampled at baseline, 10 minutes, 20 minutes, and
12 sacrifice (30 minutes).

13 A separate study was completed involving administering calcitriol subcutaneously via
14 osmotic minipump (Alzet, 2mL capacity, 10μL/hr flow rate, 0.5μg/kg/day). Aside from method
15 of administration, all other protocols were identical to the aforementioned first study. Under
16 isoflurane anesthesia, the osmotic minipump was inserted on the back dorsolaterally, and
17 subcutaneous meloxicam (2mg/kg loading, 1mg/kg maintenance) was administered pre- and
18 post-operatively for 3 days. Animals were sacrificed 9 days after pump insertion. Animals were
19 stratified into two groups based on serum calcium, phosphate, PTH, FGF-23 and bodyweight at
20 day 7. One group (N=6) received the intravenous infusion of a 300μmol phosphate spiked with
21 radiolabeled phosphate as described above. The second group (N=6) received an infusion of
22 only the tracer amount of radiolabeled phosphate, made up in saline, but lacking the phosphate
23 load.

1

2 *Tissue Harvest and Tissue Assessment Preparation:* Animals were anesthetized with isoflurane
3 (5%) and sacrificed via cardiac puncture and exsanguination. Urine was collected directly from
4 the bladder. Gastrointestinal tissue from the stomach to anus was quickly excised and separated.
5 Samples of chyme were collected from the stomach, proximal small intestine (duodenum) and
6 distal small intestine (ileum) and large intestine. Feces was collected from the distal colon.
7 Multiple somatic tissue types were collected (n=50) including various samples of arteries, veins,
8 cardiac and skeletal muscles, bone, kidney, fat, intestine, liver, pancreas, and lung. Tissues and
9 chyme were demineralized in 1N HCl for 1 week and minerals and radioactivity were measured
10 in the acid homogenate.

11

12 *Biochemical blood and urinary measurements:* Serum creatinine as well as both serum and
13 urinary calcium and phosphate were evaluated spectrophotometrically (SynergyHT Microplate
14 Reader). Creatinine was evaluated using the Jaffe method (QuantiChrom™ Creatinine Assay
15 Kit, Bioassay Systems). Serum and tissue calcium was measured using the o-cresolphthalein
16 method⁹ and free phosphate was measured using the malachite green (Sigma-Aldrich) method as
17 described by Heresztyn and Nicholson¹⁰. Plasma levels of intact PTH and C-terminal/intact FGF-
18 23 were measured by ELISA (Immunotopics Inc.).

19

20 *Radioactivity measurement and analysis:* For radioactivity assessments, serum and urine samples
21 were added to Ultima Gold AB scintillation cocktail (Perkin Elmer) and analyzed using a
22 Beckman Coulter LS 6500 multi-purpose scintillation counter. Each sample was measured twice
23 for a 1-minute count time. Corrected radioactivity was obtained by subtracting background from

1 all samples and then normalized to the amount of radioactivity ingested by each rat. Serum
2 specific activity was calculated at each time point over the course of the study (equation 1). In
3 order to transform counts/mg of tissue to an estimation of amount of phosphate accrued per
4 tissue, a time-weighted average serum specific activity was generated and was used to estimate
5 tissue phosphate accrual (equation 2) as described previously¹¹.

$$6 \quad (1) \text{ Serum Specific Activity } (\mu\text{Ci}/\text{pmol}) = \text{Serum Radioactivity } (\mu\text{Ci}/\text{uL}) / \text{Serum Phosphate} \\ 7 \quad \quad \quad (\text{mM})$$

$$8 \quad (2) \text{ Tissue PO}_4 \text{ Accrual (pmol PO}_4\text{/mg tissue)} = \text{Tissue Radioactivity } (\mu\text{Ci}/\text{mg tissue}) / \\ 9 \quad \quad \quad \text{Average Specific Activity } (\mu\text{Ci}/\text{pmol})$$

10

11 *Von Kossa Histology:* The arteries were fixed in 10X neutral phosphate-buffered saline with 4%
12 paraformaldehyde and embedded in paraffin blocks. Sections (4 μm) were stained for
13 calcification using Von Kossa's method as previously described¹². Areas of calcification
14 appeared as dark brown regions in the medial wall of the artery.

15

16 *Analysis:*

17 Text data is represented as mean \pm SD, unless otherwise indicated. The threshold for significance
18 was a p-value <0.05. All statistical tests and graph generation were done on GraphPad Prism
19 (Version 8.4). Statistics performed are outlined in detail in figure captions and table footnotes.

20

21 **Results**

22 The dietary-adenine model of CKD was confirmed by the elevated serum creatinine
23 (Table 1). In addition, CKD rats had elevated serum phosphate, PTH, and FGF-23 that was

1 exacerbated by the addition of high dietary phosphate (CKD-HP), compared to controls. A
2 chronic increase in dietary phosphate did not significantly alter any of the measured parameters
3 in control animals. Assessments of weekly increases in serum creatinine and phosphate are
4 presented in Supplementary Figure 1.

5 High dietary phosphate in CKD animals induced consistent medial layer vascular
6 calcification (VC), as indicated by substantial elevations of calcium and phosphate in both
7 central (22/23; 96%) and distal arteries (23/23, 100%). This finding was confirmed
8 histologically using von Kossa staining (Figure 1A-C). The rats fed low phosphate (CKD-LP)
9 were not significantly different from controls, with only two rats (2/23, 8.7%) developing
10 detectable VC. Taken together with circulating markers, the high dietary-phosphate group with
11 adenine-induced CKD had changes characteristic of CKD-MBD.

12 Figure 2 presents changes in circulating levels of phosphate and PTH following the oral
13 load of radiolabeled phosphate. The rats sacrificed at 2 hours did not present a different profile
14 than rats sacrificed at 6 hours (Supplementary Figure 2 and 3), as such the figure presents the
15 pooled combined profile and statistics represent combined analysis.

16 In response to the oral phosphate load, total serum phosphate increased in all groups,
17 although only significantly in CKD which occurred at 1hr and remained elevated for the
18 remainder of the 6 hr analysis. At all points, total circulating phosphate is higher in CKD-HP
19 than CKD-LP (Figure 2A), however, the chronic dietary phosphate did not impact the magnitude
20 of the absolute change in circulating phosphate at any time points (Figure 2B). Over the course
21 of the experiment, there were minimal changes in serum calcium at the measured time points
22 (Supplementary Figures 2, 3). In contrast, the chronic change in dietary phosphate altered the
23 responsiveness of PTH to the acute oral phosphate load. That is, only in the rats on low

1 phosphate diet did the PTH rise significantly from baseline in response to the acute phosphate
2 load at 1 hour (Figure 2C-D). Circulating FGF-23 was not significantly increased by the acute
3 phosphate load (Supplementary Figure 4).

4 Consistent with declining kidney function, circulating $^{33}\text{PO}_4$ elevated more in the CKD
5 rats than in the controls (Figure 2E, statistics not shown). However, there was also significant
6 impact ($p < 0.05$) of chronically increasing the dietary phosphate on the circulating $^{33}\text{PO}_4$.
7 Specifically, there was a blunted elevation of circulating $^{33}\text{PO}_4$ in the CKD-HP group at 1.5 and
8 2 hours.

9 As expected, renal phosphate clearance was decreased in CKD rats compared to controls
10 (Figure 2F). Increased dietary phosphate significantly impacted the resting urinary phosphate-to-
11 creatinine ratio in CKD, but not in controls, whereby values in the CKD-HP group is higher than
12 CKD-LP group at all time-points. There is no evidence of altered calcium excretion following
13 the oral load of phosphate in CKD animals (Supplementary Figure 5).

14 Chyme radioactivity was used as a marker of the absorption/intestinal excretion profile of
15 the acute phosphate load. Although there was no measurable impact of CKD or the chronic
16 dietary phosphate on this profile, there was an impact of time of sacrifice (Figure 2G). At 2
17 hours, there is significantly higher amount of $^{33}\text{PO}_4$ in the chyme and small intestine and very
18 little in the feces. In contrast, the opposite is true at 6 hours, at which time there is significant
19 fecal $^{33}\text{PO}_4$. The 2-hour time point reflects the status during absorption and the 6-hour time point
20 reflects the status after most intestinal absorption has already occurred.

21 Figure 2H depicts estimated amount of *de novo* phosphate across all tissues at 2 and 6
22 hours in each treatment group. Tissues were grouped according to function and/or location.
23 Supplementary Figure 7 is a grey-scale depiction of the heat map. Across all treatment groups

1 and dietary phosphate interventions, the most substantial localization occurred in the bone,
2 kidneys, liver and cardiac muscle. There was very little accrual in the fat, skeletal muscle, and
3 veins. Individual tissue graphs are depicted in Supplementary Figure 8.

4 At both 2 and 6 hours following the oral load, there was a significant impact of dietary
5 phosphate on the *de novo* phosphate accrual in the arteries, whereby accrual was markedly
6 elevated in CKD animals fed a high phosphate diet, compared to those fed a low phosphate diet
7 or control (Figure 3A). This finding was consistent throughout the vascular tree. The accrual in
8 the vasculature of the CKD animals fed a low phosphate diet, which were uncalcified, was
9 similar to that of the controls. There was no difference in accrual between 2 and 6 hours in any of
10 the treatment groups.

11 In contrast, while there was no impact of dietary phosphate on the *de novo* accrual
12 phosphate in the bone, there was an impact of CKD treatment and time of sacrifice (Figure 3B).
13 Specifically, in each group there was more accrual at 6 hours than at 2 hours, which was
14 exacerbated by CKD, likely a result of reduced clearance capacity. The arterial-to-bone accrual
15 ratio exceeds 1 in CKD-HP, indicating the accrual in the vessels per mg of tissue is higher than
16 that of bone, and at 6 hours normalizes to 1 (Figure 3C).

17 For CKD animals, pooled values at 2 and 6 hours following the oral load of radioactive
18 phosphate show that *de novo* accrual into the vessels correlates strongly with the resident tissue
19 phosphate as an indicator of VC ($r > 0.67$, $p < 0.0001$) (Figure 3D-F). At 2 hours within each
20 treatment group, a phase during which absorption is occurring, the correlation is weak and non-
21 significant. However, at 6 hours following absorption, the correlation strengthens in each group,
22 and there is a strong relationship between *de novo* phosphate and the total tissue phosphate in all
23 groups, except CON-LP.

1 In a non-CKD model of medial VC, administration of 0.5 µg/kg calcitriol for 8 days
2 resulted in hypercalcemia, transient hyperphosphatemia, suppression of PTH, and marked
3 elevation in FGF-23 (Figure 4A-D). In the subset of animals sacrificed while the stimulus was
4 still present, 8 days of calcitriol (Cx) was sufficient to generate substantial medial VC, as
5 indicated by elevations in arterial calcium and phosphate (Figure 4E-F) and confirmed
6 histologically by Von Kossa staining (Figure 4G). Thirteen days after the cessation of stimulus
7 (Post-Cx), circulating parameters of mineral metabolism had normalized, however calcification
8 was non-reduced and histologically similar to that from animals sacrificed earlier. Control
9 animals sacrificed at both timepoints were not different on any metrics assessed and were pooled
10 for all analysis (data not shown).

11 In response to a 10-minute intravenous infusion of phosphate with tracer $^{33}\text{PO}_4$, serum
12 phosphate elevated similarly in all groups (Figure 5A), and there was a reduction in calcium in
13 all groups by 20 minutes (Figure 5B). At all time-points, serum calcium was higher in the Cx
14 group, and in response to the IV phosphate, some animals had a substantial elevation in calcium
15 at 10 minutes (Figure 5B). Cx animals had a blunted elevation in $^{33}\text{PO}_4$ compared to controls and
16 Post-Cx animals (Figure 5C). Estimated tissue accrual of phosphate in response to the IV
17 challenge is presented in Figure 5D. Supplementary Figure 9 is a greyscale depiction. In a mixed
18 effects model, each tissue was compared between treatment groups (statistics not presented on
19 figure, Supplementary Table 2). There was no difference between the groups on acute accrual in
20 most tissue groups, specifically bones, kidney, adipose and veins. However, there was a
21 substantial difference in average arterial accrual, in that Cx had ~4X more deposition than
22 controls, and control and Post-Cx were not different from each other, despite Post-Cx being
23 substantially calcified (Figure 4E). Similarly, there was a correlation between VC and *de novo*

1 phosphate in both calcified groups, however there was substantially more phosphate accrual for a
2 given amount of calcification in the Cx group (Figure 5F-G).

3 In order to elucidate the role of a phosphate challenge, as opposed to non-challenged
4 movement of circulating phosphate, the IV radiolabeled phosphate infusion was compared to a
5 saline infusion spiked with $^{33}\text{PO}_4$ (Figure 6A-B). During the time-frame of the IV challenge, the
6 phosphate load stimulated urinary excretion of phosphate, that resulted in approximately 6x more
7 radioactivity excretion (Figure 6C). Subtracting the mean accrual of each tissue in the saline
8 group from the phosphate group, we generate the differential accrual as a result of the phosphate
9 challenge (Figure 6D). As expected, the kidneys exhibited the greatest difference, followed by
10 bones, central and peripheral arteries, and veins having similar differential accrual. In order to
11 assess the impact of pre-existing VC on the accrual, we see that in the setting of no-, or mild-VC,
12 the accrual is similar regardless of whether or not there was a phosphate challenge (Figure 6E-F).
13 However, as calcification progressed, the phosphate challenge preferentially deposited in the
14 vasculature.

15

16 **Discussion**

17 In the present study, we demonstrate that calcifying vasculature buffers circulating
18 phosphate in response to acute challenges, acting as an important depot during the process of
19 tissue and extracellular equilibration (Figure 7). Using a radio-labelled oral phosphate challenge
20 in a rat model of CKD-MBD, the studies revealed a blunted rise in circulating $^{33}\text{PO}_4$, that
21 associated with differential tissue deposition towards the calcifying vasculature. We confirmed
22 that tissue accrual was stimulated by an acute phosphate challenge, given that the same level of
23 deposition did not occur solely with passive disposition of circulating phosphate. The extent of

1 new transport to the calcifying vasculature correlates to the pre-existing burden of calcification,
2 and can be substantially attenuated by removing the stimulus for calcification, indicating it is
3 not a by-product of high hydroxyapatite burden, but the consequence of an active calcification
4 process.

5 The findings from this study indicate that non-renal clearance of phosphate from the
6 circulation resulting in accumulation into tissues and extracellular spaces is an important and
7 regulated process of acute phosphate homeostasis, although the specific mechanisms involved
8 were not resolved in this study. This finding is consistent with previous results demonstrating in
9 healthy animals that urinary elimination of a phosphate challenge only achieved 50% by 4 hours,
10 despite prior normalization of serum phosphate¹³. Similarly, in healthy humans, full clearance of
11 a phosphate load required approximately 120 hours¹⁴ with no impact on circulating levels.
12 Although the mechanisms responsible for prolonged, but not permanent phosphate storage, are
13 not well understood, in CKD, this would likely have unique implications due to the likelihood of
14 increased duration of storage when there is declining kidney function. In the present results,
15 serum phosphate was never significantly elevated in controls, but remained markedly elevated
16 over the entire 6 hours in CKD rats following an oral phosphate challenge. Adding tracer
17 amounts of radiolabeled phosphate to the oral load facilitated the tracking of phosphate accrued
18 in various compartments and tissues at both 2 and 6 hours following the oral challenge.
19 Assessment of radioactivity in the chyme, confirmed that active absorption was still occurring at
20 2 hours, but was nearly complete by 6 hours. Furthermore, gut absorption of phosphate was not
21 measurably altered by CKD or changes in dietary phosphate, which is similar to previous
22 findings^{15,16}.

1 In healthy animals the substantial deposition of new phosphate in the kidney cortex, liver,
2 bone and cardiac muscle at 2 hours was further increased by 6 hours despite substantial urinary
3 excretion during that time frame. In contrast, in healthy animals there was no further accrual into
4 large arteries between 2 and 6 hours, suggesting a transient deposition in this tissue.

5 In both models of VC used in this study, significant blunting of the rise in circulating
6 $^{33}\text{PO}_4$ following the oral load was associated with substantial arterial accrual. In addition,
7 increases in *de novo* phosphate accrual into blood vessels was associated with the amount of pre-
8 existing VC. When the stimulus for calcification was removed in the calcitriol-mediated VC
9 model, the phosphate no longer accrued to the same degree and the circulating $^{33}\text{PO}_4$ was similar
10 to control animals. A strength of the study is that we were able to reproduce the findings in
11 models where the stimulus and biomarker profiles being markedly different, indicating that it is
12 unlikely there is a direct role of uremic abnormalities or measured circulating factors associated
13 with mineral metabolism, with the exception of FGF-23 that was elevated in both models, and
14 reduced when the stimulus for VC was removed in the calcitriol-mediated model. Both models
15 are histologically similar and both involve osteogenic transdifferentiation¹⁷: the upregulation of
16 osteogenic markers (RUNX-2, osteocalcin) and loss of smooth muscle actin¹⁸, characteristics
17 reflected in the human condition. This transition to a bone-like phenotype may explain the
18 acquired buffering capacity. Whether this transition and subsequent acute buffering of phosphate
19 by the vasculature has physiological impacts on phosphate sensing by other organs (i.e. PTG
20 or bone) or the normal circadian rhythm of phosphate is interesting and requires further study.

21 In the CKD animals, there was a substantial increase in bone deposition of *de novo*
22 phosphate at 2 and 6 hours compared to control, which may be reflective of kidney function
23 changes. Circulating PTH was much higher in the CKD animals on high phosphate, likely

1 indicating increases in bone resorption, however this did not translate into impaired acute
2 phosphate bone storage.

3 Intermittent exposure to phosphate may be an important stimulus of negative outcomes
4 and VC progression, rather than hyperphosphatemia alone. Tani *et al.* show that chronic
5 fluctuations in dietary phosphate induced much more VC than that same load of phosphate
6 spread out consistently⁷. The current understanding of medial calcification involves phosphate
7 first entering the VMSCs through Pit-1, and then translocating to the extracellular matrix through
8 pro-calcific Ca/Pi loaded vesicles¹⁹. Vascular Pit-1 is necessary for the development of VC and
9 transdifferentiation of vascular smooth muscle cells (VSMCs) to an osteoblastic-like
10 phenotype²⁰. Transport independent PIT-1 signalling can induce osteogenic differentiation, but
11 the transport is required for extracellular matrix calcification²¹. This indicates that osteogenic
12 differentiation is not sufficient for calcification, but needs to happen in conjunction with or
13 secondary to, increased phosphate influx, potentially of the type depicted in this study. In
14 addition, the degree of Pit-1 expression appears to be, in part, dependent on dietary phosphate in
15 CKD²². Upregulation of PiT-1 alone is not sufficient for VC, and must happen in conjunction
16 with increased circulating phosphate, as demonstrated by a transgenic mouse model with
17 upregulated PiT-1, where VC was not present²³.

18 These fluctuations in phosphate have negative consequences on endothelial cells,
19 increasing oxidative stress and inflammatory responses²⁴, both of which have negative
20 consequences on cardiovascular health³. This is a potential mechanism through which more
21 frequent and longer dialysis confer positive health outcomes, although this has not been well-
22 examined as through medial VC as a mediator²⁵.

1 CKD animals fed a low phosphate diet and lacking measurable calcification had profiles
2 of vascular deposition at both the 2 and 6 hour time points that were similar to controls despite
3 the acute change in circulating phosphate similar to CKD high phosphate. In other words, the
4 circulating phosphate stimulus for deposition is similar but accrual or retention was impaired.
5 This finding is unlikely to be due to impaired cellular transport, as there is no evidence
6 suggesting a downregulation of Pit-1 in CKD with low dietary phosphate, and even uremic
7 toxins alone have been shown to upregulate Pit-1²⁶. It could however be a result of impaired
8 retention of phosphate through upregulated XPR1, the major phosphate export protein, whereby
9 dysfunction leads to brain calcifications²⁷, although it's role in VC had not been studied, or this
10 finding may indicate a successful role calcification inhibitors in making the microenvironment
11 less favourable to phosphate deposition, such as fetuin A, pyrophosphate, or matrix gla protein^{28–}
12 ³⁰.

13 The acute accrual of phosphate into the blood vessel following phosphate loading likely
14 contributes to VC propagation. Compared to the saline load, which contained similar tracer
15 levels of ³³PO₄, the phosphate challenge produced substantially more accrual into the calcified
16 vessels but not in the non-calcified vessels. This finding supports the concept that once VC is
17 initiated, it progresses quickly and potentially through a different mechanism than initiation. In
18 incident dialysis patients, only patients with pre-existing calcification had significant progression
19 over the first 18 months³¹.

20 These studies provide evidence of an important role of the calcifying vasculature in the
21 acute response to a phosphate load via a mechanism that may contribute to VC propagation. This
22 finding has important consequences for dietary management of CKD patients. Based on 2001-
23 2014 NHANES data, the average adult consumes at least twice the recommended daily intake of

1 phosphate³², whereby approximately 50% is estimated to be derived from high bioavailable
2 inorganic food additives^{33,34}. Inorganic sources, such as food additives, which are 90-100%
3 absorbed, as compared to plant- or meat-derived phosphate, which is much lower (40-69%)³⁵.
4 These inorganic sources of phosphate are quickly absorbed, leading to a more rapid flux into the
5 circulating pool. Patients with CKD and hyperphosphatemia are instructed to consume low
6 phosphate diets and prescribed intestinal phosphate binders. Phosphate binder therapy slows the
7 progression of VC, but some sub analyses have shown its most dramatic effect is on the
8 progression of pre-existing calcification³⁶.

9 Pre-existing dietary phosphate has been shown to impair sensitivity of PTH to oral
10 phosphate, which has been previously shown in healthy humans and rats, but in this study was
11 also reflected in experimental CKD [Turner et al, JBMR 2020, Revisions Submitted]³⁷. In
12 addition, in the control animals there was a very significant correlation of *de novo* deposition in
13 the vasculature at 6 hours compared to resident phosphate, despite the lack of VC, that wasn't
14 present in the LP controls. This finding potentially indicates that dietary phosphate, even in the
15 setting of healthy kidney function, alters the vascular handling of phosphate, a finding that would
16 need to be confirmed in larger studies.

17 The novel whole-body physiological approach to assessing the acute phosphate response
18 allowed comprehensive assessment of tissue deposition, and represents a powerful tool to assess
19 the sequential steps leading to VC and the impact of vascular-specific interventions. There is
20 limited evidence to suggest that calcification can regress, so nuanced assessments of activity at
21 different stages will be important for assessing treatments aimed at limiting progression. The
22 current study was limited in that we were unable to determine whether the accrual in this study

1 represents long-term deposition or temporary storage (i.e. how much of the vascular deposition
2 translated into increased accrual of VC), which is an important area of future research.

3 In summary, this study characterized the role of calcifying arteries in the acute non-renal
4 clearance of phosphate following a phosphate load in two experimental models of VC. Our data
5 indicate that calcifying arteries alter the systemic disposition of a phosphate challenge and
6 acutely deposit substantial phosphate. This study supports the importance of diet as it relates to
7 acute fluctuations of circulating phosphate and the importance of bioavailability and meal-to-
8 meal management in CKD patients as a mediator of cardiovascular risk.

1 **Acknowledgements**

2 Study Design: MET, JGEZ, BAS, MAA, RMH. Study Conduct: MET, APL, PSJ, LHL. Data
3 Collection: MET, APL, PSJ, LHL. Data Analysis: MET, MAA, RMH. Data Interpretation: MET,
4 MAA, RMH. Drafting Manuscript: MET, APL, MAA. Revising Manuscript and Content: MET,
5 APL, MAA, RMH. Approving final version of manuscript: MET, APL, PSJ, LHL, BAS, JGEZ,
6 RMH, MAA. MET takes responsibility for the integrity of the data analysis.

7

8 **Sources of Funding:** Canadian Institutes of Health Research, Queen's University. MET and
9 JGEZ are supported by Vanier Canada Graduate Scholarship.

10

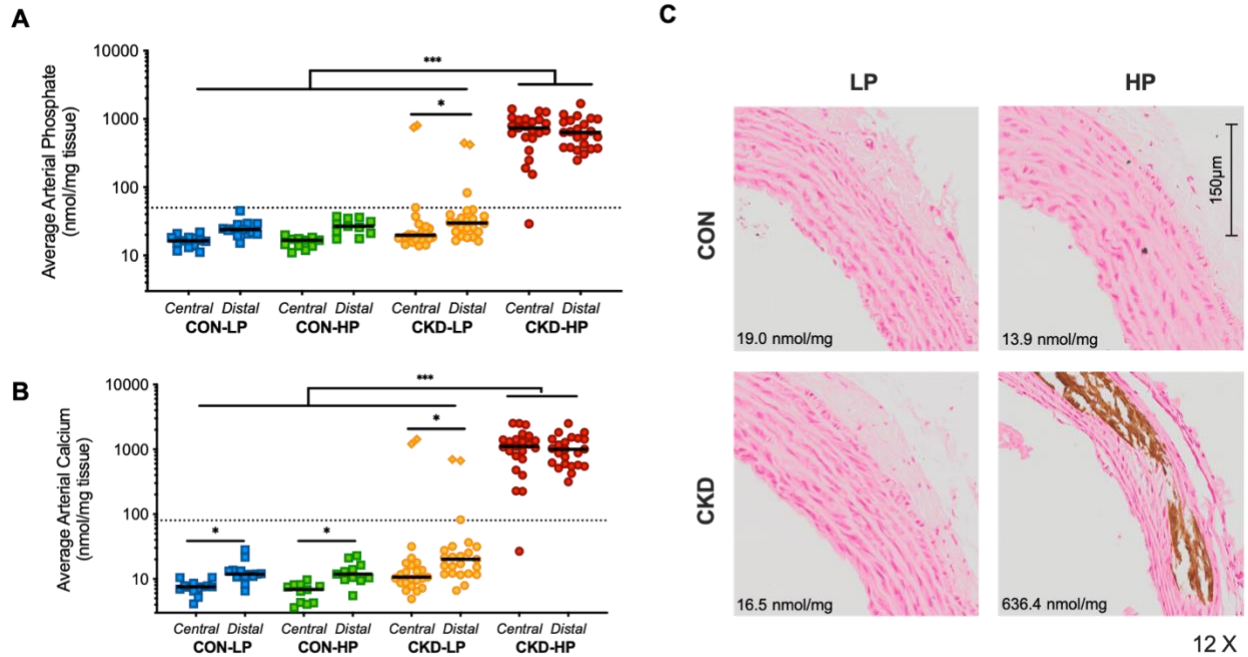
11 **Disclosures:** RMH and MAA have grant funding from OPKO Health, Renal Division for
12 projects un-related to the current manuscript. MPP has a significant relationship with OPKO
13 Health, Renal Division.

References

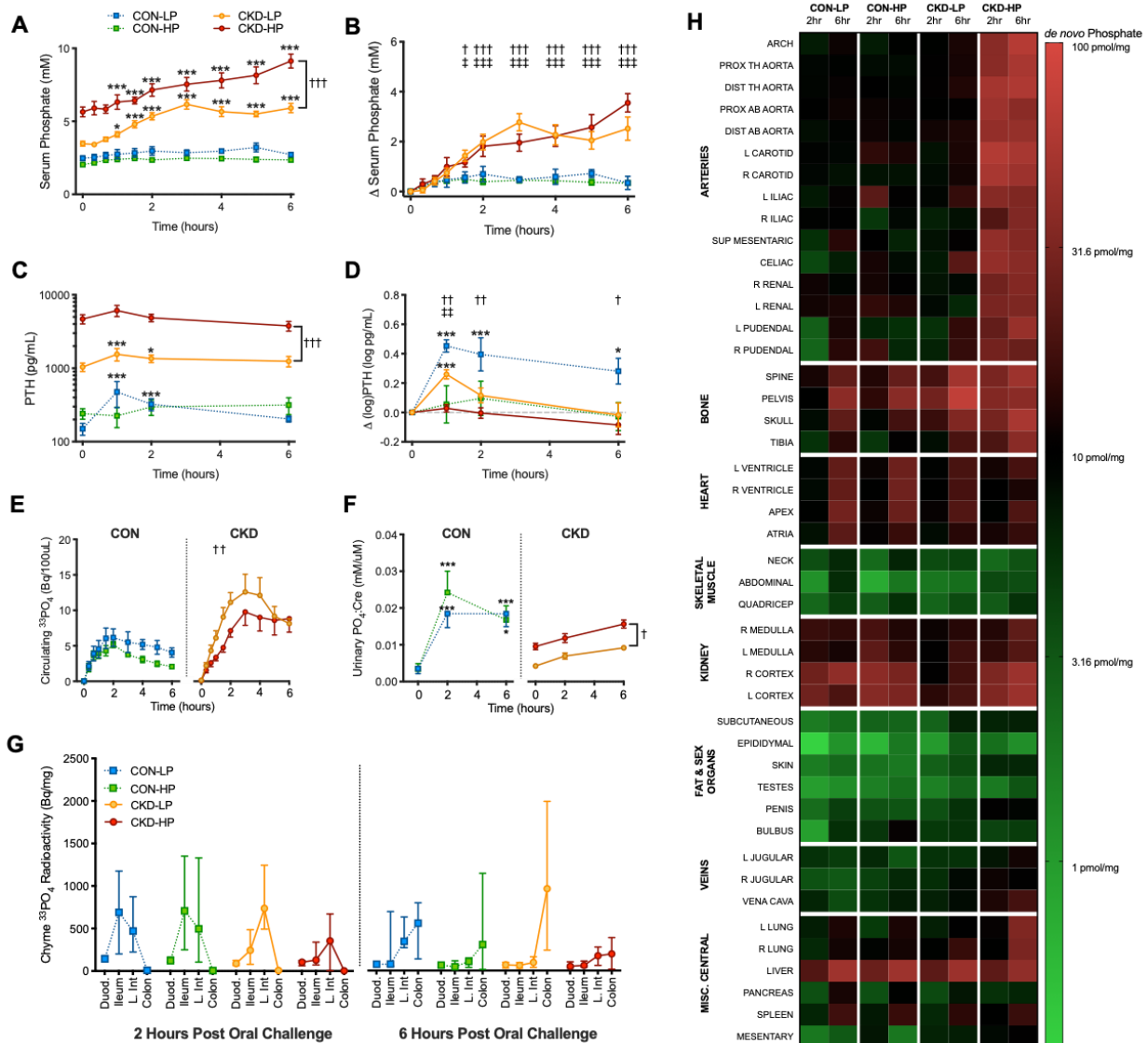
1. Detrano R, Guerci AD, Carr JJ, Bild DE, Burke G, Folsom AR, Liu K, Shea S, Szklo M, Bluemke DA, O'Leary DH, Tracy R, Watson K, Wong ND, Kronmal RA. Coronary Calcium as a Predictor of Coronary Events in Four Racial or Ethnic Groups. *New England Journal of Medicine*. 2008;358(13):1336–1345.
2. London GM, Guérin AP, Marchais SJ, Métivier F, Pannier B, Adda H. Arterial media calcification in end-stage renal disease: impact on all-cause and cardiovascular mortality. *Nephrology Dialysis Transplantation*. 2003;18(9):1731–1740.
3. Vervloet MG, Sezer S, Massy ZA, Johansson L, Cozzolino M, Fouque D. The role of phosphate in kidney disease. *Nature Reviews Nephrology*. 2016;13(1):27–38.
4. Adeney KL, Siscovick DS, Ix JH, Seliger SL, Shlipak MG, Jenny NS, Kestenbaum BR. Association of Serum Phosphate with Vascular and Valvular Calcification in Moderate CKD. *Journal of the American Society of Nephrology*. 2009;20(2):381–387.
5. Michigami T, Kawai M, Yamazaki M, Ozono K. Phosphate as a Signaling Molecule and Its Sensing Mechanism. *Physiol Rev*. 2018;98:32.
6. Turner ME, White CA, Hopman WM, Ward EC, Jeronimo PS, Adams MA, Holden RM. Impaired phosphate tolerance revealed with an acute oral challenge. *Journal of Bone and Mineral Research*. 2017.
7. Tani M, Tanaka S, Takamiya K, Sakaue M, Ito M. Effects of repetitive diet-induced fluctuations in plasma phosphorus on vascular calcification and inflammation in rats with early-stage chronic kidney disease. *Journal of Clinical Biochemistry and Nutrition*. 2020;66(2):139–145.
8. Shobeiri N, Pang J, Adams MA, Holden RM. Cardiovascular disease in an adenine-induced model of chronic kidney disease: the temporal link between vascular calcification and haemodynamic consequences. *Journal of Hypertension*. 2013;31(1):160–168.
9. Kanagasabapathy DAS. WHO: Guidelines on Standard Operating Procedures for Clinical Chemistry. 2000:113.
10. Heresztyn T, Nicholson BC. A colorimetric protein phosphatase inhibition assay for the determination of cyanobacterial peptide hepatotoxins based on the dephosphorylation of phosphovitin by recombinant protein phosphatase 1. *Environmental Toxicology*. 2001;16(3):242–252.
11. Zelt JG, Svajger BA, Quinn K, Turner ME, Lavery KJ, Shum B, Holden RM, Adams MA. Acute Tissue Mineral Deposition in Response to a Phosphate Pulse in Experimental CKD. *Journal of Bone and Mineral Research*. 2018.
12. Proudfoot D, Skepper JN, Shanahan CM, Weissberg PL. Calcification of human vascular cells in vitro is correlated with high levels of matrix Gla protein and low levels of osteopontin expression. *Arteriosclerosis, Thrombosis, and Vascular Biology*. 1998;18(3):379–388.
13. Thomas L, Bettoni C, Knöpfel T, Hernando N, Biber J, Wagner CA. Acute Adaptation to Oral or Intravenous Phosphate Requires Parathyroid Hormone. *Journal of the American Society of Nephrology*. 2017;28(3):903–914.
14. Scanni R, vonRotz M, Jehle S, Hulter HN, Krapf R. The Human Response to Acute Enteral and Parenteral Phosphate Loads. *Journal of the American Society of Nephrology*. 2014;25(12):2730–2739.
15. Vorland CJ, Lachcik PJ, Aromeh LO, Moe SM, Chen NX, Gallant KMH. Effect of dietary phosphorus intake and age on intestinal phosphorus absorption efficiency and phosphorus balance in male rats. *PLOS ONE*. 2018;13(11):e0207601.

16. Weinman EJ, Light PD, Suki WN. Gastrointestinal Phosphate Handling in CKD and Its Association With Cardiovascular Disease. *American Journal of Kidney Diseases*. 2013;62(5):1006–1011.
17. Han M-S, Che X, Cho G, Park H-R, Lim K-E, Park N-R, Jin J-S, Jung Y-K, Jeong J-H, Lee I-K, Kato S, Choi J-Y. Functional cooperation between vitamin D receptor and Runx2 in vitamin D-induced vascular calcification. *PLoS One*. 2013;8(12):e83584.
18. Lin M-E, Chen T, Leaf EM, Speer MY, Giachelli CM. Runx2 Expression in Smooth Muscle Cells Is Required for Arterial Medial Calcification in Mice. *The American Journal of Pathology*. 2015;185(7):1958–1969.
19. Yamada S, Giachelli CM. Vascular calcification in CKD-MBD: Roles for phosphate, FGF23, and Klotho. *Bone*.
20. Li Xianwu, Yang Hsueh-Ying, Giachelli Cecilia M. Role of the Sodium-Dependent Phosphate Cotransporter, Pit-1, in Vascular Smooth Muscle Cell Calcification. *Circulation Research*. 2006;98(7):905–912.
21. Chavkin NW, Jun Chia J, Crouthamel MH, Giachelli CM. Phosphate Uptake-Independent Signaling Functions of the Type III Sodium-Dependent Phosphate Transporter, PiT-1, in Vascular Smooth Muscle Cells. *Experimental cell research*. 2015;333(1):39–48.
22. Mizobuchi M, Ogata H, Hatamura I, Koiwa F, Saji F, Shiizaki K, Negi S, Kinugasa E, Ooshima A, Koshikawa S, Akizawa T. Up-regulation of Cbfa1 and Pit-1 in calcified artery of uraemic rats with severe hyperphosphataemia and secondary hyperparathyroidism. *Nephrology Dialysis Transplantation*. 2006;21(4):911–916.
23. Chande S, Ho B, Fetene J, Bergwitz C. Transgenic mouse model for conditional expression of influenza hemagglutinin-tagged human SLC20A1/PIT1. *PLOS ONE*. 2019;14(10):e0223052.
24. Watari E, Taketani Y, Kitamura T, Tanaka T, Ohminami H, Abuduli M, Harada N, Yamanaka-Okumura H, Yamamoto H, Takeda E. Fluctuating plasma phosphorus level by changes in dietary phosphorus intake induces endothelial dysfunction. *Journal of Clinical Biochemistry and Nutrition*. 2015;56(1):35–42.
25. Culleton BF, Walsh M, Klarenbach SW, Mortis G, Scott-Douglas N, Quinn RR, Tonelli M, Donnelly S, Friedrich MG, Kumar A, Mahallati H, Hemmelgarn BR, Manns BJ. Effect of Frequent Nocturnal Hemodialysis vs Conventional Hemodialysis on Left Ventricular Mass and Quality of Life: A Randomized Controlled Trial. *JAMA*. 2007;298(11):1291–1299.
26. Hénaut L, Mary A, Chillon J-M, Kamel S, Massy ZA. The Impact of Uremic Toxins on Vascular Smooth Muscle Cell Function. *Toxins*. 2018;10(6).
27. Legati A, Giovannini D, Nicolas G, López-Sánchez U, Quintáns B, Oliveira JRM, Sears RL, Ramos EM, Spiteri E, Sobrido M-J, Carracedo Á, Castro-Fernández C, Cubizolle S, Fogel BL, Goizet C, et al. Mutations in XPR1 cause primary familial brain calcification associated with altered phosphate export. *Nature Genetics*. 2015;47(6):579–581.
28. Reynolds JL, Skepper JN, McNair R, Kasama T, Gupta K, Weissberg PL, Jahnen-Dechent W, Shanahan CM. Multifunctional roles for serum protein fetuin-a in inhibition of human vascular smooth muscle cell calcification. *Journal of the American Society of Nephrology: JASN*. 2005;16(10):2920–2930.
29. Lomashvili KA, Narisawa S, Millán JL, O’Neill WC. Vascular calcification is dependent on plasma levels of pyrophosphate. *Kidney International*. 2014;85(6):1351–1356.
30. Proudfoot D, Shanahan CM. Molecular mechanisms mediating vascular calcification: role of matrix Gla protein. *Nephrology (Carlton, Vic.)*. 2006;11(5):455–461.

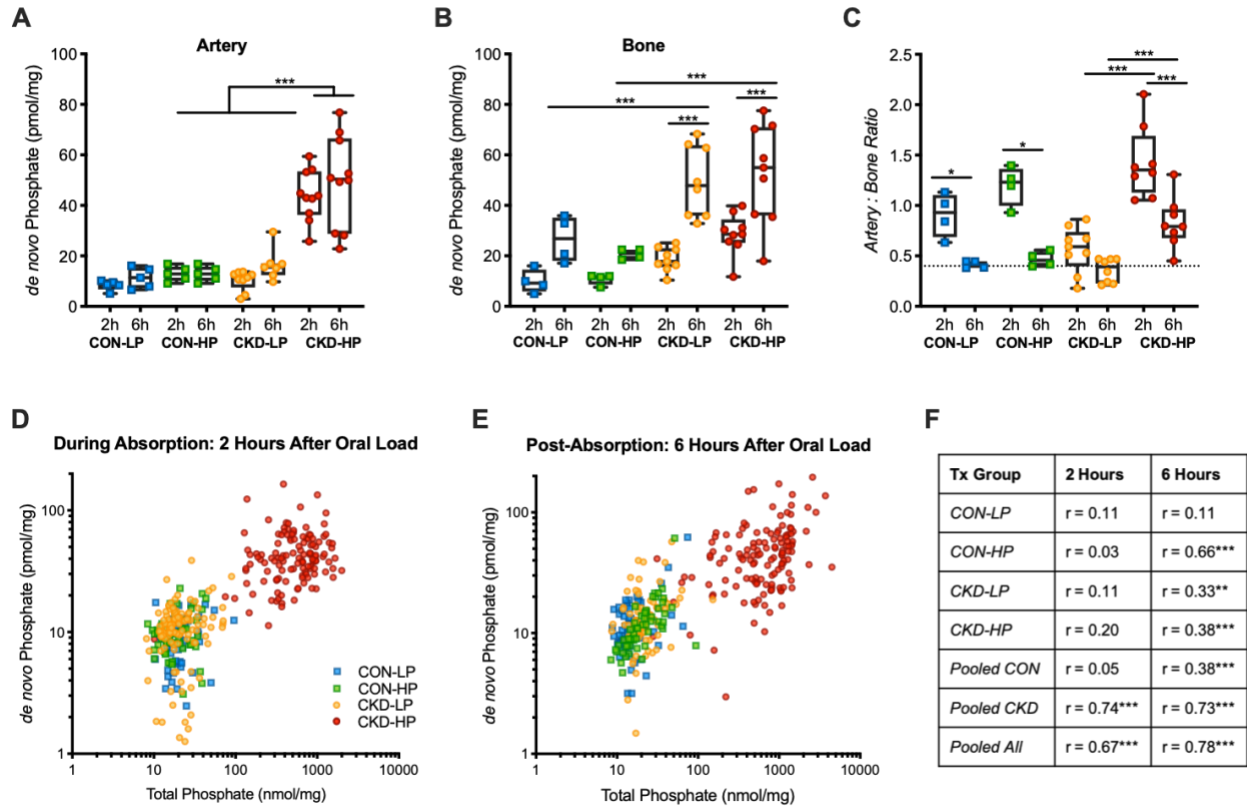
31. Block GA, Spiegel DM, Ehrlich J, Mehta R, Lindbergh J, Dreisbach A, Raggi P. Effects of sevelamer and calcium on coronary artery calcification in patients new to hemodialysis. *Kidney International*. 2005;68(4):1815–1824.
32. McClure S, Chang A, Selvin E, Rebholz C, Appel L. Dietary Sources of Phosphorus among Adults in the United States: Results from NHANES 2001–2014. *Nutrients*. 2017;9(2):95.
33. Gutiérrez OM, Luzuriaga-McPherson A, Lin Y, Gilbert LC, Ha S-W, Beck GR. Impact of Phosphorus-Based Food Additives on Bone and Mineral Metabolism. *The Journal of Clinical Endocrinology & Metabolism*. 2015;100(11):4264–4271.
34. Hill Gallant KM. Studying dietary phosphorus intake: the challenge of when a gram is not a gram. *The American Journal of Clinical Nutrition*. 2015;102(2):237–238.
35. Adema AY, de Borst MH, Ter Wee PM, Vervloet MG, NIGRAM Consortium. Dietary and pharmacological modification of fibroblast growth factor-23 in chronic kidney disease. *Journal of Renal Nutrition: The Official Journal of the Council on Renal Nutrition of the National Kidney Foundation*. 2014;24(3):143–150.
36. Chertow GM, Burke SK, Raggi P, Treat to Goal Working Group. Sevelamer attenuates the progression of coronary and aortic calcification in hemodialysis patients. *Kidney International*. 2002;62(1):245–252.
37. Turner ME, Mazetti T, Ward EC, Munroe J, Jeronimo PS, Adams MA, Holden RM. Diets high in inorganic phosphate alter acute calcium homeostasis and PTH sensitivity in healthy rats and humans. (**Journal of Bone and Mineral Research - Revisions Submitted**)



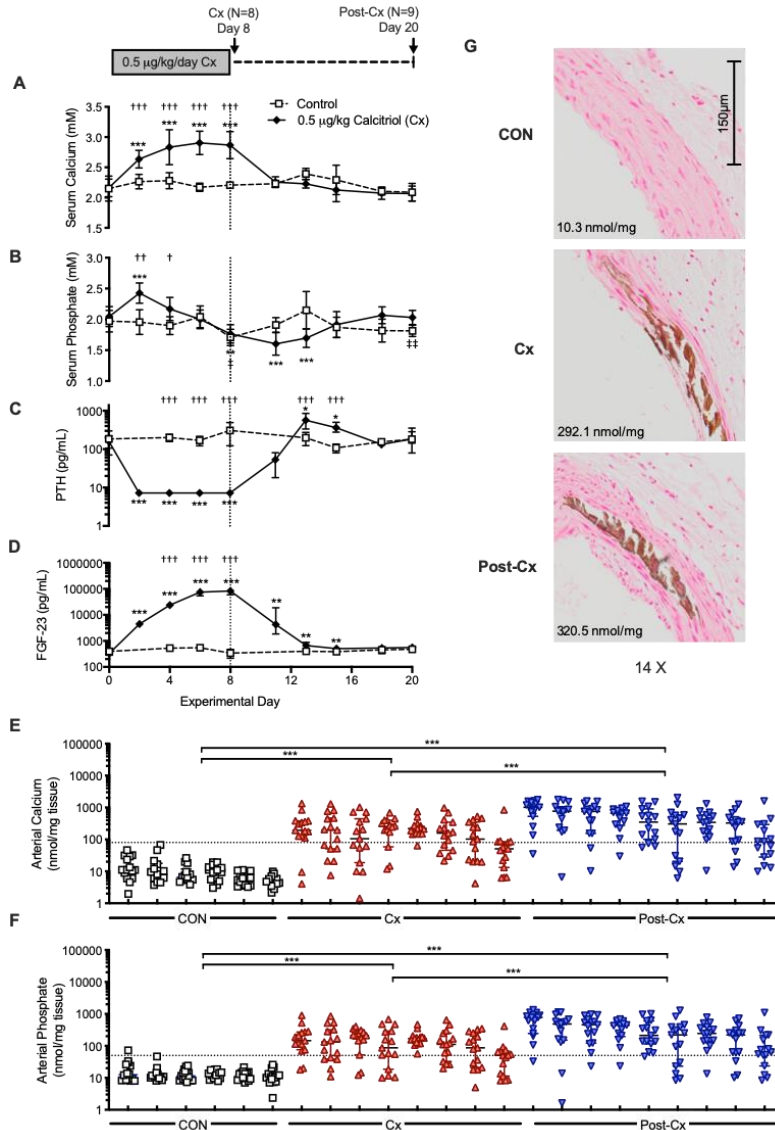
1
2 **Figure 1: Increased dietary phosphate induces medial vascular calcification in arterial tissue in**
3 **experimental CKD. (A)** Arterial phosphate and **(B)** calcium per mg of wet weight tissue. Line at median.
4 Each data point represents the mean of central (N=5) and peripheral (N=10) vessels in each rat. Dotted
5 line at 50 ng/mg tissue phosphate and 80 ng/mg tissue calcium, the approximate mineral levels needed to
6 detect vascular calcification histologically via von Kossa staining. Three-way ANOVA on log-transformed
7 data with *post hoc* Tukey-corrected multiple comparisons. * $p < 0.05$, ** $p < 0.01$ *** $p < 0.001$. **(C)**
8 Representative visible aortic medial calcification indicated by von Kossa phosphate staining in only CKD-
9 HP. Tissue phosphate indicated on image.



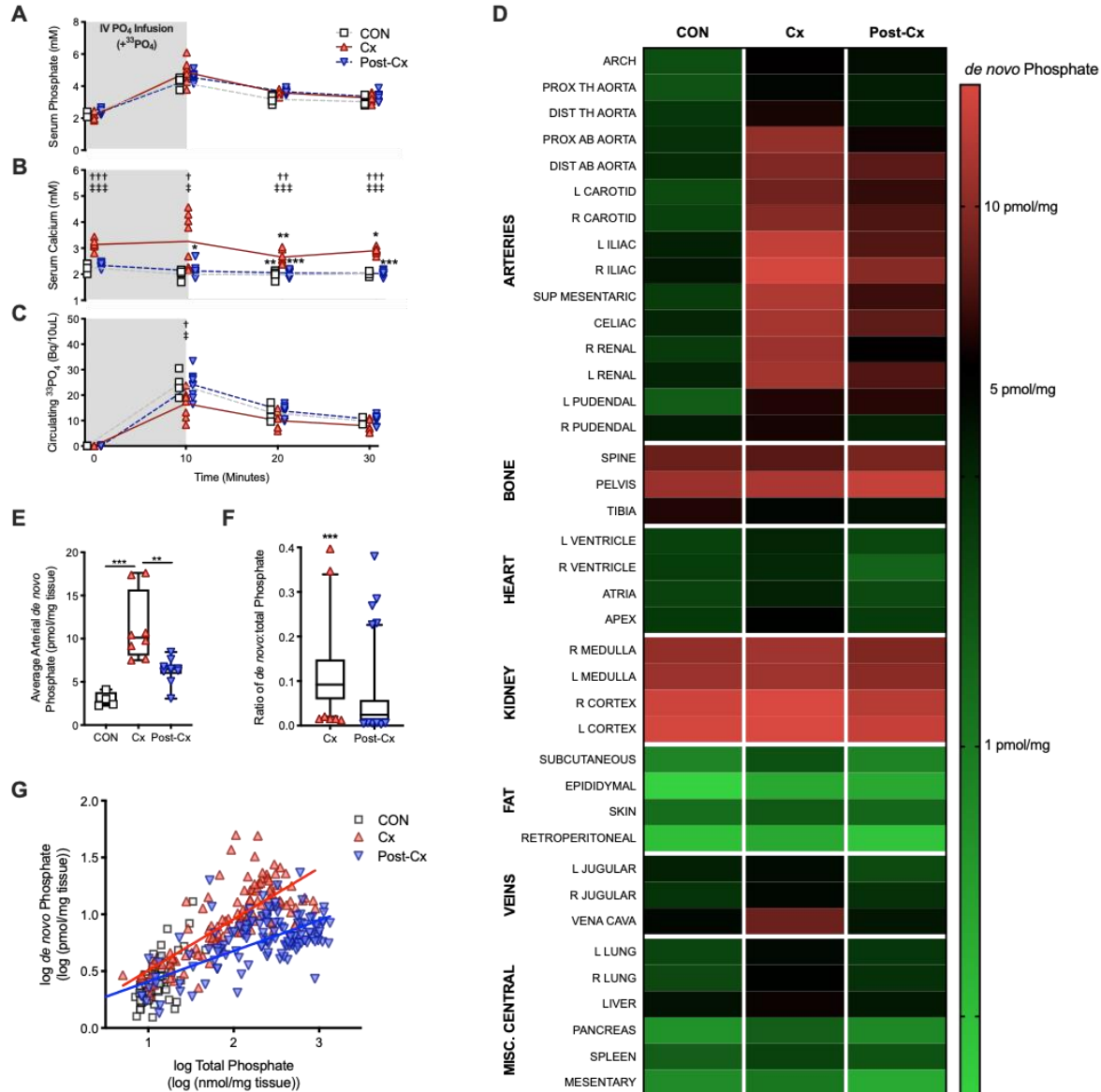
1
 2 **Figure 2: Acute response and tissue deposition to radiolabeled phosphate challenge altered by**
 3 **dietary phosphate in experimental model of CKD (A)** Circulating total phosphate, **(B)** absolute change
 4 in total phosphate, **(C)** circulating PTH, **(D)** absolute change in log-transformed PTH, **(E)** circulating $^{33}\text{PO}_4$
 5 per 100 μL of serum, and **(F)** urinary phosphate: creatinine ratio. Repeated measures mixed effects model
 6 analysis with *post hoc* tests evaluating within-group differences from time 0 (Dunnett's correction; *
 7 $p < 0.05$, * $p < 0.01$, *** $p < 0.001$) and between group differences comparing CKD-LP to CON-LP (†) and
 8 CKD-HP to CON-HP (‡) at each time point, unless indicated otherwise (Tukey correction; † $p < 0.05$, ††
 9 $p < 0.001$). Data expressed as mean \pm SEM. Comparisons of PTH panel C, evaluated on log-transformed
 10 data. **(G)** Change in the profile of radioactive phosphate along the gastrointestinal tract at 2 hours and 6
 11 hours following an oral load of radioactive phosphate. Radiolabeled phosphate load along intestinal tract
 12 indicates at 2 hours following oral load, small intestinal absorption is still occurring, and has finished by 6
 13 hours in all groups. **(H)** Experimental CKD and dietary phosphate alter tissue disposition of an oral load of
 14 radiolabeled phosphate. *De novo* tissue phosphate accrual in various tissues across the body at 2 and 6
 15 hours following oral load grouped by tissue type. The heatmap coloration represents the amount of *de*
 16 *nov*o phosphate accumulated per mg of wet-weight tissue on a logarithmically-transformed scale. Arteries
 17 sorted by external diameter. For full tissue list see supplementary methods.



1
2
3 **Figure 3: Calcified vascular tissue is a depot of *de novo* phosphate in the setting of experimental**
4 **CKD and high dietary phosphate.** Comparison of *de novo* phosphate deposition in (A) arteries, (B)
5 bone, and (C) the ratio artery:bone at 2 and 6 hours after the oral phosphate. Each data point represents
6 the pooled average of the 15 arterial or 4 bone samples for each individual rat. Dotted line on pane C
7 represents pooled control means at 6 hours. Three-way ANOVA with *post hoc* Sidak-corrected multiple
8 comparisons. *p<0.05, **p<0.01 *** p<0.001 between data-sets that differed only by one variable. (A)
9 CKD intervention (p<0.001), dietary phosphate (p<0.001), and their interaction (p<0.05) were significant
10 sources of variation. (B) CKD intervention (p<0.001), time of sacrifice (p<0.001), and their interaction
11 (p<0.05), but not dietary phosphate, were significant sources of variation. (C) The interaction of dietary
12 phosphate and CKD intervention (p<0.001), time of sacrifice (p<0.001), dietary phosphate (p<0.001), and
13 their interaction (p<0.05) were significant sources of variation. (D-F) *De novo* phosphate accumulation
14 correlates with present vascular calcification. Change in *de novo* arterial phosphate accumulation as a
15 function of total tissue phosphate at 2 hours (D) and 6 hours (E) following the oral load. Each data point is
16 from a single artery sample (15 different artery samples x 51 animals = 795 data points). Spearman
17 correlation r-values of each group and pooled groups (F). *p<0.05, **p<0.01, ****p<0.001.

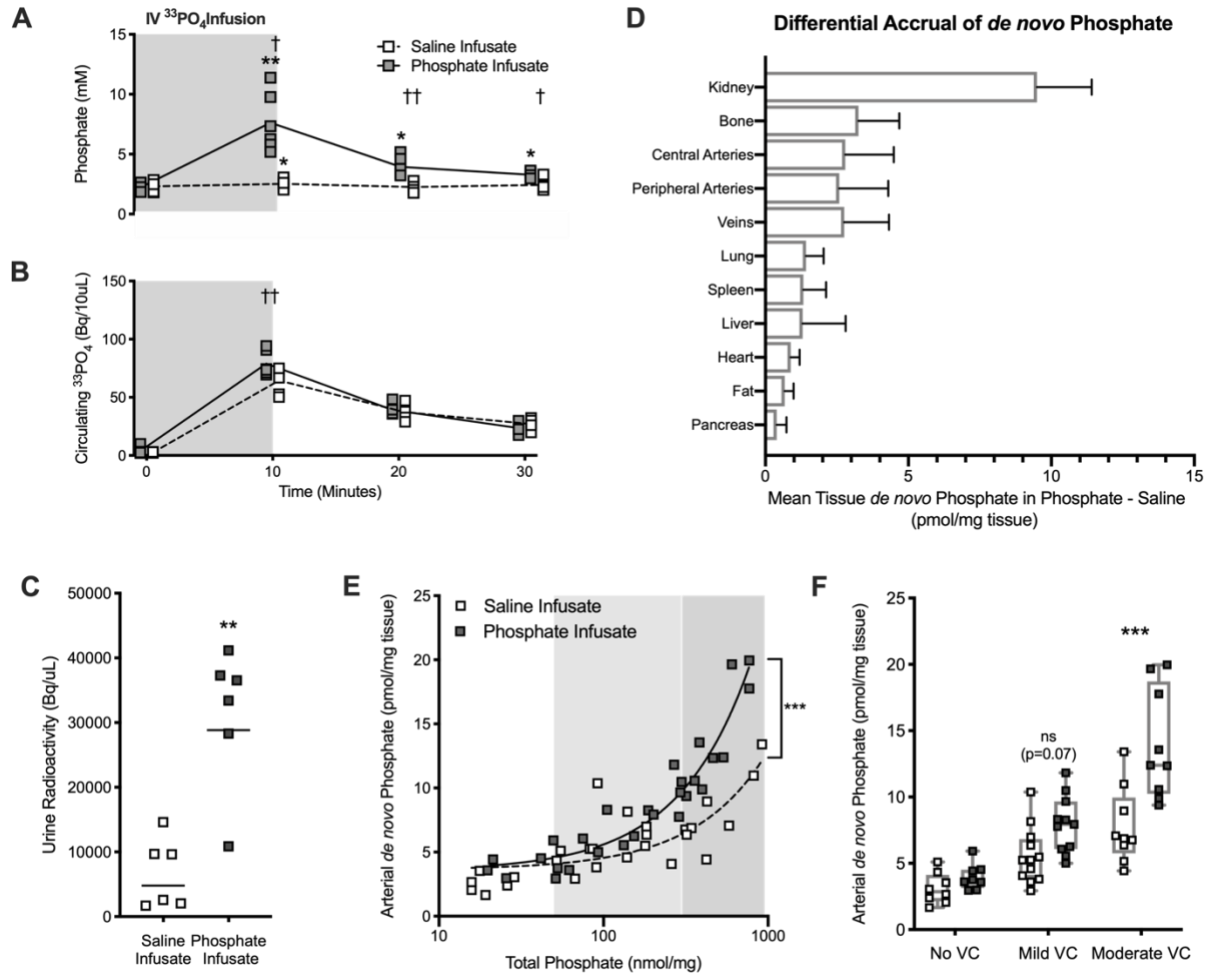


1
 2 **Figure 4: Persistence of vascular calcification in non-CKD model after removal of the calcification**
 3 **stimulus and normalization of circulating markers.** Perturbations of circulating **(A)** calcium, **(B)**
 4 phosphate, **(C)** PTH, **(D)** FGF-23 following dosage of calcitriol (0.5 µg/kg/day) for 8 rats (Cx). After
 5 cessation of treatment for 12 days, circulating parameters largely returned to normal (Post-Cx). Repeated
 6 measures mixed effects model analysis with *post hoc* tests evaluating within-group differences from time
 7 0 (Dunnett's correction; * p < 0.05, ** p < 0.01, *** p < 0.001) and between group differences comparing Cx to
 8 Post-Cx (†) (Tukey correction; † p < 0.05, †† p < 0.001). Data expressed as mean ± SD (A-B) or median
 9 IQR (C-D). Comparisons of PTH and FGF-23 evaluated on log-transformed data. Persistent vascular
 10 calcification, as indicated by **(E)** arterial calcium and **(F)** phosphate after removal of stimulus. Each
 11 column represents an animal, and each data-point a vascular tissue measured. Dotted line at 50 ng/mg
 12 tissue phosphate and 80 ng/mg tissue calcium, the mineral levels needed to detect vascular calcification
 13 histologically via von Kossa staining. Two-way ANOVA on log-transformed data with *post hoc* Tukey-
 14 corrected multiple comparisons. ***p < 0.001. **(G)** Representative visible medial calcification indicated by
 15 Von Kossa phosphate staining in both the Cx and Post-Cx rats.



1
 2 **Figure 5: Presence of a stimulus for calcification differentially impacts acute deposition in**
 3 **calcified vessels (A)** Circulating phosphate, **(B)** calcium, and **(C)** radiolabeled $^{33}\text{PO}_4$ during and after the
 4 IV infusion of a radiolabeled phosphate load. Repeated measures two-way ANOVA with *post hoc* tests
 5 comparing Cx – CON(†), and Post-Cx to CON(‡) (Tukey correction; † $p < 0.05$, ††† $p < 0.001$) and
 6 evaluating within-group differences from time 0 (Dunnett's correction; * $p < 0.05$, *p < 0.01 , *** $p < 0.001$). At
 7 no time point was Post-Cx different than CON. At all time-points, serum phosphate and circulating $^{33}\text{PO}_4$
 8 was higher than at baseline. Line at mean. **(D)** *De novo* tissue phosphate accrual in various tissues
 9 across the body grouped by tissue type. The heat map coloration represents the amount of *de novo*
 10 phosphate accumulated per mg of wet-weight tissue on a logarithmically-transformed scale. Arteries
 11 sorted by external diameter. For full tissue list see supplementary methods. **(E)** Average arterial *de novo*
 12 phosphate for each animal. Kruskal-Wallis with *post hoc* Dunn's multiple comparison test (** $p < 0.01$,
 13 *** $p < 0.001$). **(F)** Ratio of *de novo* arterial phosphate to total arterial phosphate for each vessel. Median,
 14 IQR, 95% CI shown. Data points outside 95% CI plotted. Mann-Whitney test (** $p < 0.01$). *De novo*
 15 phosphate accumulation in arteries plotted against total tissue phosphate following IV infusion. Each data
 16 point is from a single artery sample. Log-log linear regression plotted (Cx: $R_2 = 0.58$, $y = 0.45x + 0.05$, Post-
 17 Cx: $R_2 = 0.40$, $y = 0.27x + 0.14$).

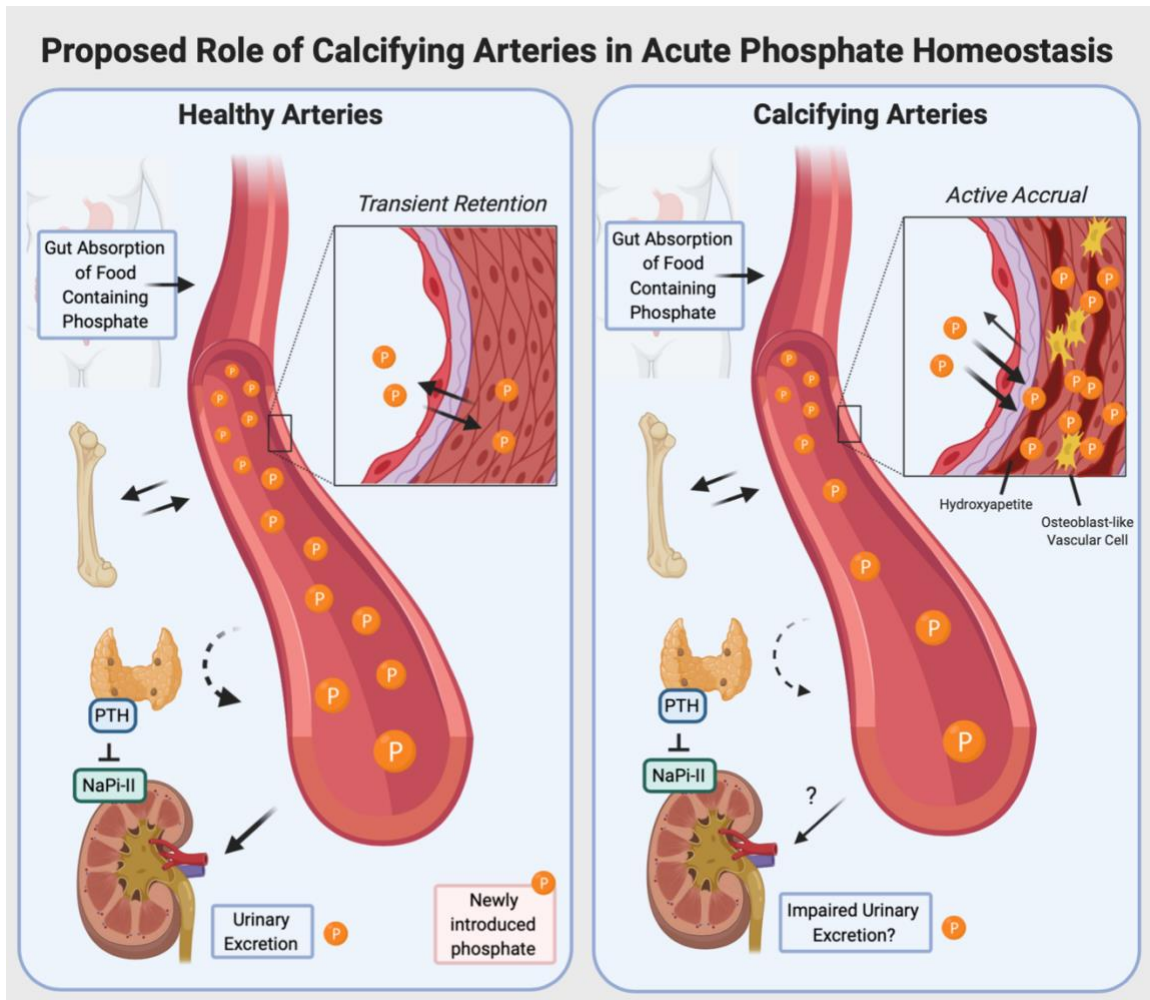
1



2

3 **Figure 6: Acute phosphate acts as a stimulus for differential vascular deposition in calcified**
 4 **vessels only (A)** Circulating phosphate and **(B)** radiolabeled $^{33}\text{PO}_4$ during and after the IV infusion of
 5 either a radiolabeled phosphate load or saline with tracer. Repeated measures two-way ANOVA with *post*
 6 *hoc* tests comparing within-group differences from time 0 (Dunnett's correction; * $p < 0.05$, * $p < 0.01$,
 7 *** $p < 0.001$) and between infusates at each time point (Sidak correction; † $p < 0.05$, ††† $p < 0.001$). Line at
 8 mean. **(C)** Urine radioactivity compared using Mann-Whitney test, line at geometric mean. **(D)** Differential
 9 *de novo* phosphate accrual in phosphate versus saline infusion. Mean tissue *de novo* phosphate in saline
 10 infusion group subtracted from phosphate group. Mean SD. **(E)** *De novo* phosphate accumulation in
 11 arteries plotted against total tissue phosphate following IV infusion. Each data point is from a single
 12 central artery sample. Linear regression plotted (Phosphate: $R_2 = 0.91$, $y = 0.021x + 3.5$, Saline: $R_2 = 0.60$,
 13 $y = 0.009x + 3.6$). Slopes of lines are significantly different $p < 0.001$. **(F)** Calcified vasculature selectively
 14 accrues more phosphate acutely. Degree of calcification binned according to no VC ($< 50 \text{ nmol/mg}$), mild
 15 VC ($50\text{-}300 \text{ nmol/mg}$), and moderate VC ($> 300 \text{ nmol/mg}$). Two-way ANOVA with *post hoc* Sidak-corrected
 16 comparisons between infusates (** $p < 0.01$).

17



1

2

3

4

5

Figure 7: Proposed conceptual framework describing the role of calcifying vasculature in the response to an acute challenge of oral phosphate (i.e. a meal) and consequences.

1 **Table 1: CKD-MBD Rat Model Characteristics at Sacrifice**

2

Treatment Group	Creatinine (μM)	PO_4 (mM)	Ca (mM)	PTH (pg/mL)	FGF23 (pg/mL)	Bodyweight (g)
CKD-LP	441.4 \pm 100.0 4a, 4b	3.74 \pm 0.80 2a, 4b	2.79 \pm 0.52	930 [542,1479] 4a, 4b	4192 [3322,7226] 4a, 4b	465 \pm 27 3a, 1b
CKD-HP	512.4 \pm 166.6 4a, 4b	5.05 \pm 0.98 4a, 4b, 4c	2.47 \pm 0.72	3100 [2497,6090] 4a, 4b, 4c	68176 [47507,85767] 4a, 4b, 4c	411 \pm 25 4a, 4b, 4c
CON-LP	41.7 \pm 8.8	2.47 \pm 0.62	2.51 \pm 0.28	131 [99, 220]	326[306,383]	506 \pm 22
CON-HP	42.8 \pm 10.4	2.04 \pm 0.23	2.57 \pm 0.31	243 [109, 296]	306[287,320]	497 \pm 28
<i>CKD Intervention</i>	***	***	ns	***	***	***
<i>Dietary Phosphate</i>	ns	***	ns	***	***	***
<i>Interaction</i>	ns	***	ns	***	***	***

3

4 Two-way ANOVA with Sidak's multiple comparisons test. ^aDifference from CON-LP ^bDifference from CON-HP ^cDifference from
5 CKD-LP. PTH. 1b: p<0.05, 2a: p<0.01. 3a: p<0.001, 4a or 4b or 4c: p<0.0001. PTH/FGF-23 represented as median [IQR] and
6 statistics performed on normalized log-transformed data. Values for phosphate, calcium, PTH reflect directly prior to oral phosphate
7 load. Significant sources of variation as identified by two-way ANOVA bottom three rows. ***p<0.001

8